

# USING THE LAP-SHEAR TEST TO MEASURE POLYMER COMPOSITE INTERFACIAL STRENGTH

I. Swentek\*, J.T. Wood

Mechanical and Materials Engineering,  
The University of Western Ontario, London, Ontario, Canada

\* Corresponding author ([iswentek@uwo.ca](mailto:iswentek@uwo.ca))

**Keywords:** *Lap-shear, interfacial strength, polymer matrix composites (PMCs), TOF SIMS*

## 1 Abstract

A modified lap–shear test is presented which can quickly provide a direct measurement of the interfacial strength of a glass reinforced thermoset composite. The test is sensitive to both polymer curing conditions and chemical modification of the interface. Epoxy and polyester are each bonded to both clean glass and silane-coated glass to measure their interfacial shear strengths. The fractured interfaces are examined at an atomic level using time-of-flight secondary ion mass spectrometry to determine the location and rheology of fracture. Finally, the experimental results are validated against traditional interfacial strength measurement methods. This test is a simple way to assess the final mechanical properties of a polymer composite – something not previously feasible.

## 2 Background

The transportation industry requires structural materials that are as light as possible. Glass fibre reinforced polymers (GFRP) are among the best engineering materials with high specific strength and stiffness [1]. The use of GFRP materials in structural automotive applications requires numerical models capable of predicting not only elastic, but also inelastic behaviour to model crashworthiness [2-3].

The elastic behaviour of GFRP is well understood and easily calculated [1]. The inelastic behaviour of a fibre reinforced polymer is predictable with knowledge of the geometry, the mechanical response of the polymer, the reinforcement, and importantly, the interface between these constituents [4-7]. Current techniques to measure the interfacial strength of a composite system are indirect methods and require complex sample preparation [8-14].

A relatively simple and repeatable test has been developed to measure the interfacial properties

directly [15]. The test was first validated using a glass/epoxy system, for which the data maintained close agreement with values reported in the available literature [16-21]. The test is now extended to a glass/polyester system, to demonstrate the utility in mass produced composite components for the automotive industry by the sheet moulding compound (SMC) process [22].

## 3 Experimental Procedure

### 3.1 Polymer characterization

Two polymers were used to examine the interfacial properties over a range of interfacial conditions. A two-part epoxy: CLR 1180 resin and CLH 6560 hardener was procured from Crosslink Technologies Inc. The polyester, T320-70, was sourced from AOC. A peroxide-based polymerization initiator, Luperox DDM-9, was added to the polyester to aid curing. The standard cure conditions were four hours at 60C and 80C for the epoxy and polyester respectively. Mechanical properties of both polymers were determined after EN ISO 527.

### 3.2 Lap-shear Testing

To test the interface of a glass fibre reinforced composite, a model system is constructed. Lap-shear joints, schematically shown in Figure 1, were fabricated following [15]. Glass slides are selected as the substrate and cleaned and baked before use. A teflon mask is inserted during fabrication to restrict the geometry and reduce stress concentrations at the joint edges. The addition of near-thru slits allowed the mask to be removed prior to testing without causing damage to the bonded area.

Two types of interfaces were examined in this study: the neat polymer bonded to clean glass and the neat polymer bonded to glass coated in a silane coupling agent, similar to those used in industry. The silane coupling agent was selected for its applicability to

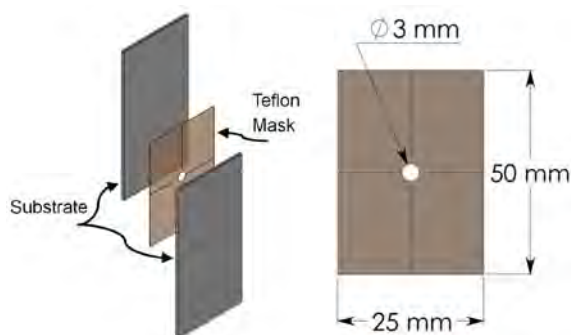


Fig.1. Schematic diagram of a lap-shear specimen with dimensioned Teflon mask

these particular thermosetting polymer systems, 3-(Trimethoxysilyl)propyl methacrylate, also called Z6030, from Dow Corning. The silane was diluted to 2% in a 95% ethanol/5% water solution before the cleaned glass slides were coated. The solution pH was controlled to the range of 4.5-5.5 with glacial acetic acid. The coated slides were cured at 100C for two hours before sample assembly.

To mitigate sample variance, a test series consisted of 10 identically created samples. The mode of loading was investigated by adjusting the Teflon mask thickness. The effects of cure temperature were also tested, though only for the epoxy. For consistency, all samples were tested at room temperature (22C) within 24 hours of creation to minimize any effects of polymer aging.

An Instron 8804 load frame with a 5 kN load cell was used to perform the lap-shear testing. The polymer-glass interface is subjected to shear by subjecting the specimens to a compressive load at a constant displacement rate of 0.5 mm/min. A 12.5 mm gauge extensometer was attached to capture strain data, as seen in Figure 2. To prevent the glass substrate from fracturing in the steel grips and to help with alignment, rubber spacers were inserted between the grip face and the substrate.

### 3.3 Surface Analysis

To verify the location and distribution of the interfacial fracture, time-of-flight secondary ion mass spectrometry (ToF SIMS) was employed. Baseline spectra were taken of each of the neat surfaces (glass, silane coated glass, epoxy, and polyester) to determine fingerprint regions for subsequent surface comparison. To reduce batch variance, all samples used for the surface analysis were produced at the same time and were tested

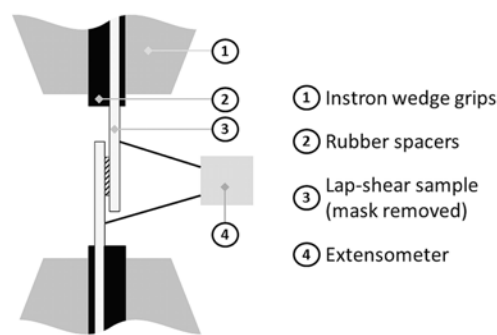


Fig.2. Schematic diagram of the lap-shear compression test setup.

within 12 hours of fabrication to minimize exposure to contaminants.

An ION-TOF (Gmbh) TOF-SIMS IV equipped with a Bismuth cluster liquid metal ion source was used. A 25 keV Bi<sup>3+</sup> cluster primary ion beam pulsed at 10 kHz was used to bombard the sample surface to generate secondary ions. The positive or negative secondary ions, one polarity selected at a time, were extracted from the sample surface. The ions were mass separated and detected via a reflection-type of time-of-flight analyzer, allowing parallel detection of ion fragments having a mass/charge ratio ( $m/z$ ) up to ~900 within each cycle (100  $\mu$ s). A pulsed, low energy electron flood was used to neutralize sample charging. Ion mass spectra were collected at  $128 \times 128$  pixels over an area of  $500 \mu\text{m} \times 500 \mu\text{m}$  for 60 s. The collected spectra were calibrated using the mass/charge peaks for hydrogen and carbon.

## 4 Results

### 4.1 Mechanical Testing

Selected mechanical properties of the respective polymers are reported in Table 1. Though both polymers are thermosets, the polyester is brittle, with an average strain-to-failure of 2.7 %, while the epoxy is partially ductile with an average strain-to-failure of 7.7%. The densities of each polymer were determined by the Archimedes method.

Table 1. Reported mechanical properties for the epoxy and polyester with standard deviations.

Property	Epoxy	Polyester
Young's Mod. (GPa)	2.00 ( $\pm 0.03$ )	1.60 ( $\pm 0.06$ )
Yield Stress (MPa)	21.7 ( $\pm 1$ )	16.0 ( $\pm 1$ )
Tensile Stress (MPa)	48.7 ( $\pm 1$ )	28.5 ( $\pm 1$ )
Poisson's Ratio	0.30 ( $\pm 0.01$ )	0.28 ( $\pm 0.01$ )
Density ( $\text{g}/\text{cm}^3$ )	1.16 ( $\pm 0.01$ )	1.21 ( $\pm 0.01$ )

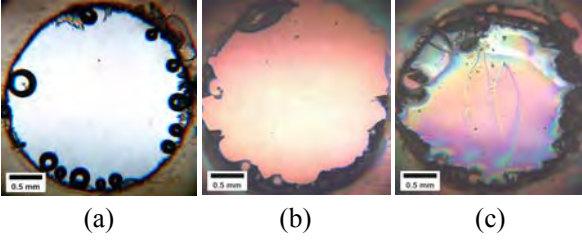


Fig. 3. Epoxy lap-shear sample (without coupling agent) a) prior to fracture; b) and c) post fracture under polarized light. Images have been rotated and aligned to ease comparison; the scale bar is 0.5 mm.

From the lap-shear experiments, the average shear stress is calculated per Eqn. 1, below, from the initial area. Here the assumption is made that the substrate does not bend during testing so the shear stress is assumed uniform. The area is corrected by subtracting a small amount to account for entrapped air during the fabrication process. Seen in Figure 3a, small air bubbles are present in the fabricated lap-shear sample, which reduce the initial bonded area. The clean surface from Figure 3b would indicate that fracture occurs cleanly at the glass-polymer interface.

$$\bar{\tau} = F/A_o \quad (1)$$

The shear strain is calculated as:

$$\gamma = \arctan(\delta/t_o) \quad (2)$$

where  $\delta$  is the vertical displacement of the lap-shear sample, obtained from the extensometer, and  $t_o$  is the initial thickness of the polymer disk. The shear strain is assumed constant across the face of the polymer disk, which is valid so long as  $E_{\text{substrate}} \gg E_{\text{polymer}}$ . A small correction is made to account for the elastic loading of the substrate above and below the lap joint, assuming a rectangular area, with length equal to the extensometer gauge. The maximum correction is less than 2.5% of the strain value at fracture load.

Typical results from the lap-shear experiments are presented in Figures 4 and 5 for the epoxy and polyester samples respectively. The mask thickness for both sets of data was 0.18 mm. The interfacial strength is taken as the peak value from the stress-strain curve. The initial slope of the shear stress-strain curves closely follows the expected shear modulus, though standard tensile testing yielded less data spread.

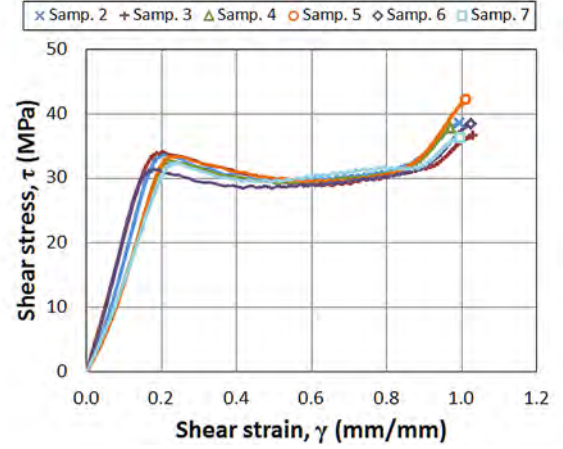


Fig. 4. Typical shear stress-strain curves for epoxy bonded to silane coated glass.

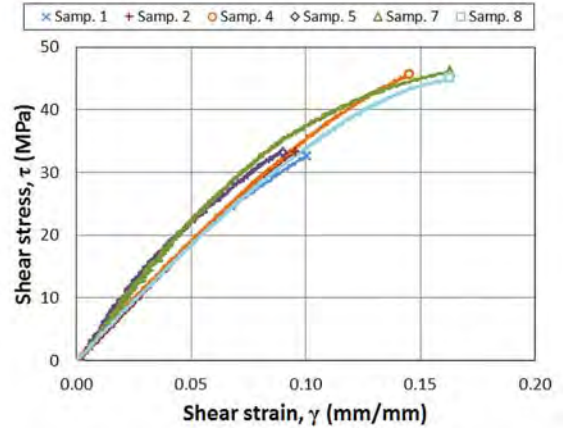


Fig. 5. Typical shear stress-strain curves for polyester bonded to silane coated glass.

Controlling the disk thickness, via different mask thicknesses, also controlled the mode of loading. During testing, the offset nature of the lap joint causes a moment about the center of the sample. In turn, a resultant normal stress is created, distributed along the face of the polymer disk. As the disk thickness is increased, the resultant normal load increases, lowering the measured shear stress at failure. Data for both polymers is shown in Figure 6. Disks with an aspect ratio (thickness/ diameter) greater than unity are not recommended as additional failure modes may be incurred and keeping the substrate plates parallel during testing becomes challenging.

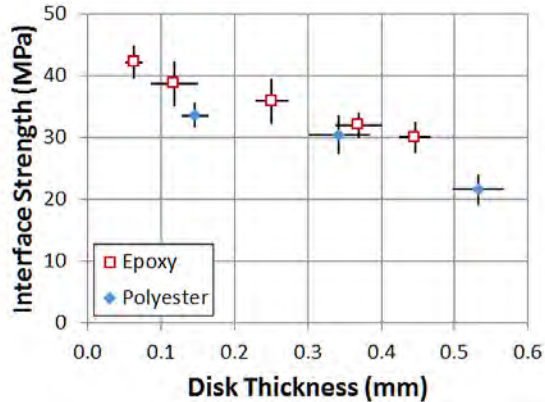


Fig. 6. Interfacial shear strength as a function of polymer disk thickness.

Further, the polymer cure conditions are expected to substantially influence the composite interfacial strength. The results for the glass/epoxy system are shown in Figure 7 for several different cure temperatures. Though the interfacial strength increases with the cure temperature, the polymer becomes increasingly brittle and the work of fracture decreases at high temperature cure. The work of fracture is the integrated area under the stress-strain curve.

#### 4.2 Interfacial Chemistry

To examine the interfacial behavior of the GFRP systems, surface analysis was conducted on the uncoated, coated, and post-fracture glass surfaces using time-of-flight secondary ion mass spectrometry. The resulting data analysis provides insight into the location and morphology of fracture.

After collecting mass spectra for the four surfaces: clean glass, coated glass, epoxy, and polyester, unique mass/charge peaks were manually identified. Table 2 lists some of the unique ion mass/charge ratios for each of the surfaces. The charge was calibrated to unity, so the mass/charge ratio can be directly interpreted as ion mass.

Table 2. Unique ‘fingerprint’ ion mass/charge ratios for the four analyzed surfaces.

Surface	Positive ions	Negative ions
Clean glass	28, 63, 91	28
Coated glass	73, 147	85
Epoxy	57, 58, 91, 135, 165	35, 93, 133, 211
Polyester	71, 82, 99, 112, 140, 157, 215	27, 57, 71, 115, 155, 173, 271

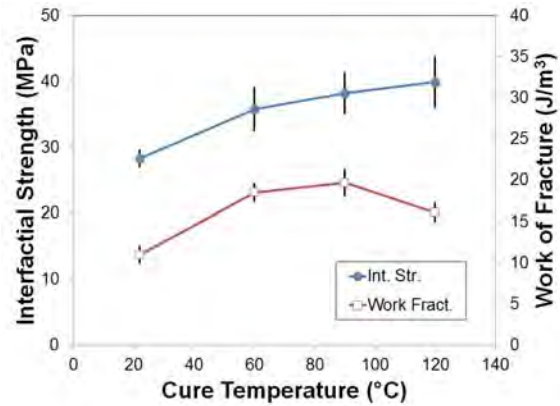


Fig. 7. Shear strength and work of fracture for the glass/epoxy system as related to cure temperature.

Smaller ion masses can be easily identified by atomic mass, as there are limited possibilities. For example, the ion mass of 28 can be identified as Silicon. Higher ion masses require a prior knowledge of the molecular structure and additional testing to accurately identify the composition from the many possible atomic mass combinations. The purpose of this study was not to determine composition; thus, unique peaks will be identified solely by their ion mass number.

Fractured surfaces were examined in light of the identified fingerprint mass peaks that each material exhibited. Figure 8 presents enlarged sections of the mass spectra for ion masses unique to clean glass and epoxy on each side of a fractured interface. The spectra have been normalized with respect to the total ion count, to accommodate direct comparison

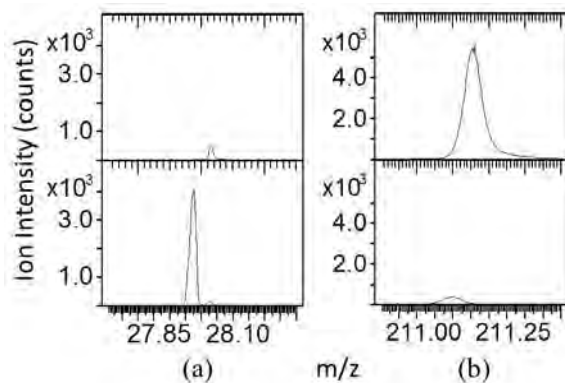


Fig. 8. Normalized negative-ion counts at a) glass and b) epoxy fingerprint peaks. Upper and lower frames correspond respectively to one side of a fractured epoxy/glass interface.

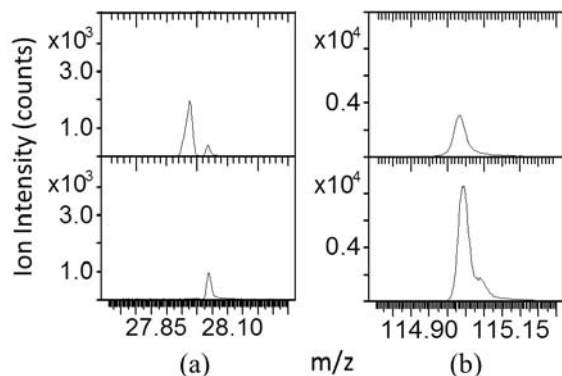


Fig. 9. Normalized negative-ion counts at a) glass and b) polyester fingerprint peaks. Upper and lower frames correspond respectively to one side of a fractured polyester/glass interface.

On one side of the fractured interface, there exist no measurable ions from the glass, while the epoxy ions are fully present. The other side contains the glass ions and only a small presence of epoxy is detected. A similar result is obtained with the polyester/glass interface, seen in Figure 9, though there is more of a polyester presence on the glass-side of the fractured interface. The physical representation of these fracture surfaces can be seen in Figure 3b and 3c, where one side of a fracture is visually void of polymer, while the other side retains the polymer disk.

## 5 Discussion

### 5.1 Interfacial Failure Location

By rastering the ion beam across an inspected surface, the distribution of ions can be obtained. Recording the ion count at each location gives an understanding of the surface morphology of the fracture surface using the resulting image intensity. The presented images are not normalized so that intensity can be directly compared. Though the images are taken of fractured surfaces, the locations selected for ToF SIMS analysis do not necessarily align between the image sets.

Figure 10 provides a visualization of the distribution of ions on the fracture surface of a clean glass/epoxy sample. The epoxy ions, masses 93 and 211, indicate even distribution of the epoxy on both surfaces, while the relative amounts on each surface are substantially different. The glass indicator, ion mass 28, is nearly absent from Figure 10a, which is to be expected on the epoxy-side of the fractured interface.

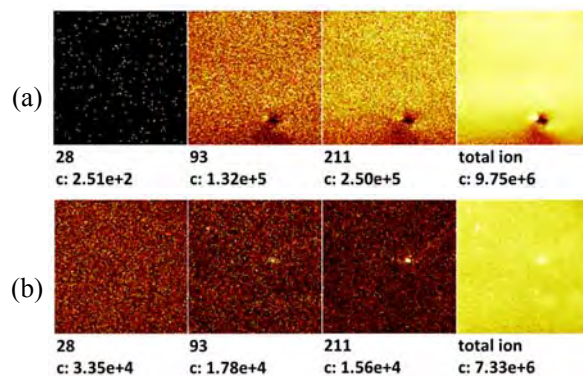


Fig. 10. Negative-ion distributions for the two halves of a fractured glass/epoxy interface. The ion mass and ion count are below each image.

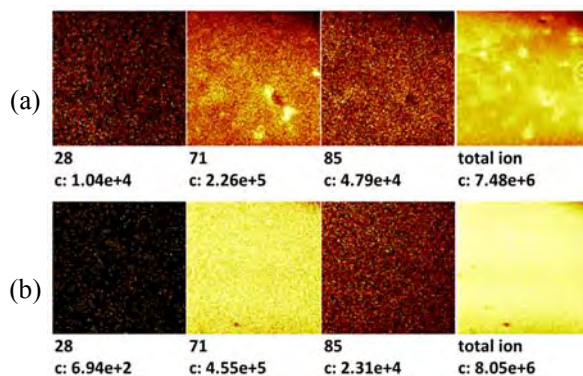


Fig. 11. Negative-ion distributions for the two halves of a fractured polyester/coated glass interface. The ion mass and ion count are below each image.

The even distribution of epoxy ions in figure 10b indicates a uniform fracture, void of areas of retained polymer. The dark spot in figure 10a is a small bubble just below the epoxy surface causing a warp in the surface, which demonstrates the sensitivity of the measurement to geometric irregularity. The failure of the clean glass and polymer interface is seen to occur right at the interface, as opposed to in either the substrate or the polymer; true for both epoxy and polyester. This would substantiate the hypotheses that predominate fracture occurs at the chemical interface between the glass and polymer.

The fracture of a silane coated glass and polyester interface is presented in Figure 11. The silane ion marker, mass 85, is present on both sides of the interface. In Figure 11b, the presence of glass is negligible, while the polyester is most noticeable (mass 71), which is again expected for the side of fracture with the retained polymer disk.

Together, the low presence of glass and distributions of the polyester and the coupling agent suggest that fracture occurs between the coupling agent and the polymer. The epoxy exhibited similar results: the coupling agent is both strongly bonded to the glass and evenly distributed across the glass surface.

## 5.2 Interfacial Failure Quantization

The lap-shear data from Figures 4 and 5 indicate a brittle interface from the sharp fracture. The highest point for each curve is taken as the value of the interfacial shear strength. The epoxy is seen to have substantial plastic deformation, with the presence of a plateau region in the shear stress-strain curves, and high shear strain at failure. The collected experimental results for the interfacial strengths are presented in Fig. 12.

The polyester displays higher standard deviation as compared to the epoxy due to lower sample size. Epoxy with the Z6030 silane coated glass showed statistically similar strength to that of clean glass, while the Z6040 coated glass had increased strength. With both polymers, substantial gains to both interfacial strength and work of fracture are possible through the use of a coupling agent. The importance of properly pairing a polymer and coupling agent to achieve improved properties cannot be understated.

Performing multiple test series for different disk thicknesses, the interfacial shear strength can be linearly extrapolated; refer to Figure 6. A separate test, as described in [15] was used to measure the interfacial normal strength for both polymers. Together, these values are reported in Table 3.

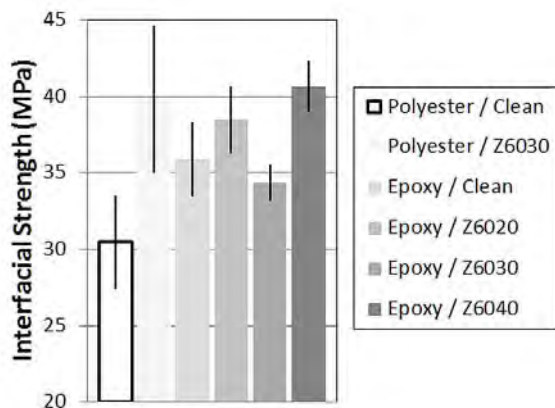


Fig.12. Interfacial shear strengths for epoxy and polyester bonded to both clean and silane coated glass [15].

Table 3. Interfacial strengths for epoxy and polyester bonded to clean glass, with standard deviations.

	Shear (MPa)	Normal (MPa)
Epoxy/glass	42.9 ( $\pm 2.9$ )	24.5 ( $\pm 1.1$ )
Polyester/glass	37.0 ( $\pm 2.5$ )	15.7 ( $\pm 0.9$ )

The utility of the reported shear and normal interfacial strength values is derived from their application in numerical simulations. The Hashin criterion provided in Eqn. 3, has been demonstrated as an appropriate interfacial failure criterion for thermosetting polymers [23]. Failure occurs when the combination shear and normal loading ratios are greater than or equal to unity.

$$\left(\frac{\tau}{\tau_f}\right)^2 + \left(\frac{\sigma}{\sigma_f}\right)^2 \geq 1 \quad (3)$$

The subscript ‘f’ represents the failure stress. The results from all the polymer/clean glass lap-shear experiments are plotted against the Hashin criterion in Fig. 13. Good agreement is observed between theoretical and experimental failure.

Though not enumerated here, the simplicity and ease of constructing a suitable interfacial system allows for testing impacts from other areas of composite development. Fillers, fibre treatments, polymer additives and processing conditions are all application targets for such a test as described. Also possible to test are the direct impacts of chemical exposure, service environment, and fatigue on the interfacial strength.

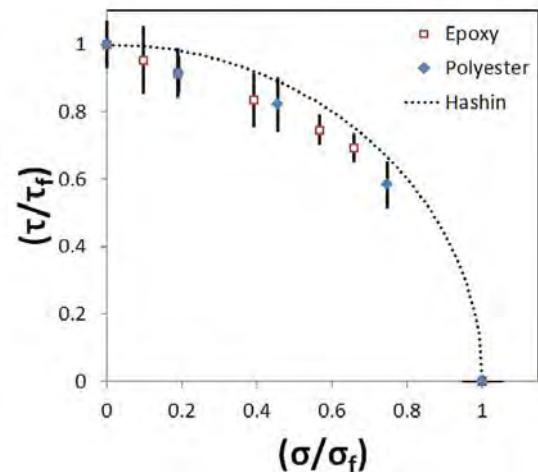


Fig. 13. Experimental interfacial failure for epoxy and polyester systems plotted with the Hashin failure criteria

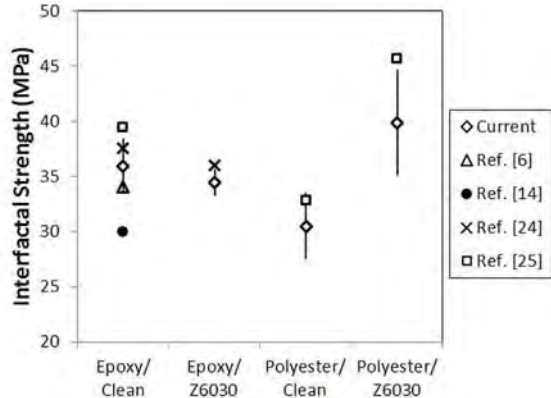


Fig. 14. Comparison of interfacial shear strengths against similar composite systems found in the literature.

As a final confidence check, the reported interfacial shear strengths are compared against similar material systems from the literature in Figure 14.

## 6 Summary

A simple test for interfacial strength based on a macroscopic model system has been developed and analyzed. Fracture surfaces were analyzed to determine the surface morphology and fracture location. Fracture of neat polymer on clean glass occurs at the chemical interface of the glass/polymer composite, while fracture of silane coated glass composites occurs between the polymer and the silane coupling agent.

The test represents a direct method of obtaining the interfacial strength of a polymer composite system. The test has been shown to be consistent with established experimental techniques which infer interfacial properties. Furthermore, the test has been shown to be sensitive to variations in interfacial chemistry and resin curing conditions.

## 7 Acknowledgements

We would like to acknowledge the contribution of Dr. Heng-Yong Ni in performing the ToF SIMS measurements. This research was funded by the International Composites Research Center under ORF grant #RE-05-057.

## References

[1] Hull D., Clyne T.W. (1996) *An introduction to composite materials, 2nd ed.* Cambridge, New York.

[2] Cheah L. and Heywood J. (2010) "Meeting U.S. passenger vehicle fuel economy standards in 2016 and beyond". *Energy Policy*, Vol. 39, No. 2, pp. 454-466.

[3] Jacob G.C., et al (2002) "Energy absorption in polymer composites for automotive crashworthiness". *J. Compos. Mater.*, Vol. 36, No. 7, pp. 813-850. Doi:10.1177/0021998302036007164

[4] Hinton M.J., et al (eds) (2004) *Failure criteria in fibre reinforced polymer composites: the world-wide failure exercise.* Elsevier, San Diego.

[5] Tay T.E., et al (2008) "Progressive failure analysis of composites". *J. Compos. Mater.*, Vol. 42, No. 18, pp. 1921-1966. Doi:10.1177/0021998308093912

[6] Chua P.S. and Piggott M.R. (1985) "The glass fibre-polymer interface: II – work of fracture and shear stresses". *Compos. Sci. Technol.*, Vol. 22, No. 2, pp. 107-119. Doi:10.1016/0266-3538(85)90079-X

[7] Kim J.K. and Mai Y.W. (1998) *Engineered interfaces in fibre reinforced composites.* Elsevier, New York.

[8] Zhandarov S. and Mäder E. (2005) "Characterization of fiber/matrix interface strength: applicability of different tests, approaches and parameters". *Compos. Sci. Technol.*, Vol. 65, No. 1, pp. 149-160. Doi:10.1016/j.compscitech.2004.07.003

[9] Kim J.K., et al (1992) "Interfacial debonding and fibre pull-out stresses: part I. a critical comparison of existing theories with experiments". *J. Mater. Sci.*, Vol. 27, No. 12, pp. 3143-3154. Doi:10.1007/BF01116004

[10] Zhou L.M., et al (1992) "Interfacial debonding and fibre pull-out stresses: part II. a new model based on the fracture mechanics approach". *J. Mater. Sci.*, Vol. 27, No. 12, pp. 3155-3166. Doi:10.1007/BF01116005

[11] Gupta V., et al (1993) "Calculation, measurement and control of interface strength in composites". *J. Am. Ceram. Soc.*, Vol. 76, No. 2, pp. 305-315. Doi:10.1111/j.1151-2916.1993.tb03784.x

[12] Hsueh C.H. (1990) "Interfacial debonding and fibre pull-out stresses of fibre-reinforced composites". *Mater. Sci. Eng. A-Struct.*, Vol. 123, No. 1, pp. 1-11. Doi:10.1016/0921-5093(90)90203-F

[13] Zhou L., et al (1993) "Micromechanical characteristics of fibre/matrix interfaces". *Compos. Sci. Technol.*, Vol. 48, No. 1-4, pp. 227-236. Doi:10.1016/0266-3538(93)90140-C

[14] Zhou X., et al (2001) "Interfacial properties of polymer composites measured by push-out and fragmentation tests". *Compos. A*, Vol. 32, No. 11, pp. 1543-1551. Doi:10.1016/S1359-835X(01)00018-5

[15] Swentek I.N. and Wood J.T. (2013) "Measuring polymer composite interfacial strength". *Compos. Part B-Eng.* (submitted) pp. 1-19.

[16] Favre J.P. and Jacques D. (1990) "Stress transfer by shear in carbon fiber model composites: part I results of single fiber fragmentation tests with thermosetting

- resins". *J. Mater. Sci.*, Vol. 25, No. 2, pp. 1373-1380.  
Doi:10.1007/BF00585453
- [17] Bruce T.P. (2011) "Mechanistic mixed-mode failure criterion for continuous fiber-polymer composites". Ph.D. thesis. University of Western Ontario, London.
- [18] Sitterle V.B. (2008) "A modified lap test to more accurately estimate interfacial shear strength of bonded tissues". *J. Biomech.*, Vol. 41, No. 15, pp. 3260-3264. Doi:10.1016/j.jbiomech.2008.09.006
- [19] Laird II G., and Kennedy T.C. (1995) "Poisson's ratio and the interfacial behaviour of composite materials". *Composites*, Vol. 26, No. 12, pp. 887-889. Doi:10.1016/0010-4361(95)90882-Z
- [20] Buehler M.J., Keten S., and Ackbarow T. (2008) "Theoretical and computational hierarchical nanomechanics of protein materials: deformation and fracture". *Prog. Mater. Sci.*, Vol. 53, No. 8, pp. 1101-1241. Doi:10.1016/j.pmatsci.2008.06.002
- [21] Park S., Jin J., and Lee J., (2000) "Influence of silane coupling agents on the surface energetics of glass fibers and mechanical interfacial properties of glass fiber-reinforced composites". *J. Adhesion Sci. Technol.*, Vol. 14, No. 13, pp. 1677-1689. Doi:10.1163/156856100742483
- [22] Kalpakjian S. and Schmid S.R. (2007) *Manufacturing Processes for Engineering Materials, 5th ed.*, Prentice Hall, New Jersey, Chap. 10.
- [23] Hashin Z, Rotem A (1973) "A fatigue failure criterion for fibre reinforced materials". *J. Compos. Mater.*, Vol. 7, No. 4, pp. 448-464. Doi:10.1177/002199837300700404
- [24] Tanoglu M, et al (2001) "The effects of glass-fiber sizings on the strength and energy absorption of the fiber/matrix interphase under high loading rates". *Compos. Sci. Technol.*, Vol. 61, No. 2, pp. 205-220. Doi:10.1016/S0266-3538(00)00195-0
- [25] Yeung P, Broutman LJ (1978) "The effect of glass-resin interface strength on the impact strength of fiber reinforced plastics". *Polym. Eng. Sci.*, Vol. 18, No. 2, pp. 62-72. Doi:10.1002/pen.760180203